

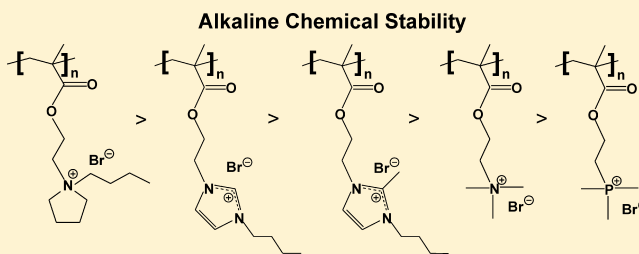
# Alkaline Chemical Stability of Polymerized Ionic Liquids with Various Cations

Kelly M. Meek and Yossef A. Elabd\*

Department of Chemical Engineering, Texas A&amp;M University, College Station, Texas 77843, United States

## Supporting Information

**ABSTRACT:** The success of long-lasting low-cost (non-platinum) alkaline fuel cells is dependent on the development of anion exchange membranes (electrolyte separator) with high alkaline chemical stability. In this study, a series of methacrylate-based polymerized ionic liquids (PILs) were synthesized with various covalently attached cations: butylimidazolium, butylmethylimidazolium, trimethylammonium, pentamethylguanidinium, butylpyrrolidinium, and trimethylphosphonium. The alkaline chemical stability of these PILs was examined in tandem with their analogous ionic salts: 1-butyl-3-methylimidazolium chloride, 1-butyl-2,3-dimethylimidazolium chloride, tetramethylammonium chloride, benzyltrimethylammonium chloride, hexamethylguanidinium chloride, 1,1-butylmethylpyrrolidinium chloride, and tetramethylphosphonium chloride. The degradation mechanisms and extent of degradation were quantified using  $^1\text{H}$  NMR spectroscopy at various pHs (in  $\text{D}_2\text{O}$ ), and temperature. The PILs with imidazolium and pyrrolidinium cations showed enhanced chemical stability relative to the PILs with ammonium and phosphonium cations. Interestingly, direct correlations were not observed between the PILs and their analogous small molecule ionic salts; significant degradation was observed in imidazolium ionic salts, most notably at high temperature/high pH conditions, while the pyrrolidinium-, ammonium-, and phosphonium-based ionic salts showed no degradation under any of the conditions examined. Additionally, results on the imidazolium ionic salts showed that methyl substitution in the C2 position limited the ring-opening degradation reaction, whereas the PIL with the unsubstituted imidazolium actually showed higher chemical stability relative to its substituted PIL counterpart. Overall, the alkaline chemical stability of the PILs in this study showed no correlation to that of their analogous small molecule ionic salts, suggesting that alkaline chemical stability studies on small molecules may not provide a solid basis for evaluating alkaline stability in polymers, counter to the hypothesis in many previous studies.



## INTRODUCTION

Alkaline fuel cells (AFCs) employing solid-state anion exchange membranes (AEMs) as electrolytes are of great interest, as they produce high power densities at low operating temperatures ( $<200\text{ }^\circ\text{C}$ ) and enable the use of non-platinum electrodes (e.g., nickel), significantly reducing cost relative to proton exchange membrane fuel cells.<sup>1</sup> Recently, a number of AEMs have been developed for the AFC.<sup>2–30</sup> One of the critical challenges limiting the wide scale use of solid-state AFCs is the alkaline chemical stability of the AEM. Degradation of the covalently tethered cationic groups, as well as the polymer backbone, may be triggered by the high nucleophilicity and basicity of  $\text{OH}^-$  ions, which are produced in an AFC and transported through the AEM. Although degradation of the polymer backbone should be considered, it is generally accepted as more chemically stable than the cation. Further investigations are necessary to determine the most promising cations for long-term stability in the presence of hydroxide in order to achieve long-lasting AFC performance.

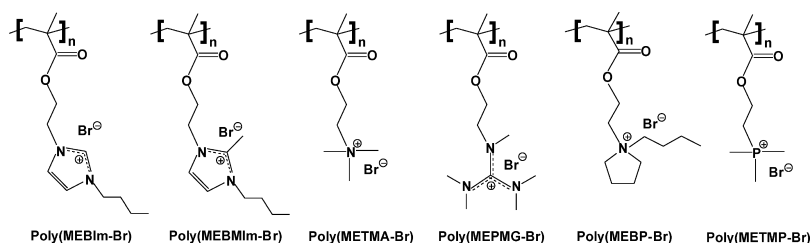
The benzyltrimethylammonium (BTMA) cation is the most frequently employed cation in AEMs due to ease of functionalization, high conductivity and thermal stability, and adequate alkaline stability on short time scales in hydrated

conditions.<sup>13–19</sup> However, BTMA is known to degrade under alkaline conditions over time by nucleophilic substitution, thus leading to the consideration of other cations that may show improved alkaline chemical stability. Alternative AEMs with other cations, such as imidazolium,<sup>2–12</sup> phosphonium,<sup>23–25</sup> guanidinium,<sup>26–29</sup> and pyrrolidinium,<sup>30</sup> have recently been investigated. Specifically, many recent stability studies on AEMs for AFCs have focused on monitoring ionic conductivity over a designated period of time after an AEM is immersed in a concentrated alkaline solution, as a means of measuring chemical stability of the AEM under specific test conditions.<sup>5–7,20,24</sup> Hibbs<sup>20</sup> compared various benzylic cations on the polyphenylene backbone: BTMA, pentamethylguanidinium, and *N*-methylimidazolium. The resonance stabilized cations, benzylic pentamethylguanidinium and *N*-methylimidazolium, showed  $>25\%$  decrease in ionic conductivity and ion exchange capacity (IEC) after 1 day in 4 M KOH at  $90\text{ }^\circ\text{C}$ , while the BTMA showed  $\sim 33\%$  decrease after 14 days. No change in IEC and only  $\sim 5\%$  decrease in conductivity were observed under

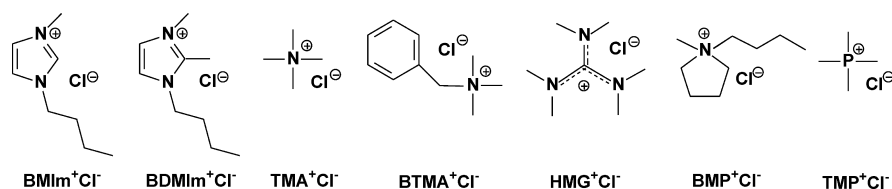
Received: June 5, 2015

Revised: September 9, 2015

Scheme 1. Chemical Structures of PIL Homopolymers with Various Pendant Cations



Scheme 2. Chemical Structures of Ionic Salts



the same conditions for 14 days when a hexamethylene spacer was included between the polymer backbone and BTMA, demonstrating the importance of not only cation type but also how the cation is attached to the polymer backbone. Coates and co-workers<sup>24</sup> showed the potential benefits of a sterically crowded cation by exploring the stability of tetrakis(dialkylamino)phosphonium-functionalized polyethylene relative to BTMA-functionalized polyethylene. The bulky phosphonium-based cation outperformed the BTMA cation, maintaining its conductivity over a 20 week period in 15 M KOH at 22 °C and experiencing only a small decrease in conductivity (from 22 to 18 mS cm<sup>-1</sup>) over 22 days in 1 M KOH at 80 °C. Prior to this study, Yan and co-workers<sup>25</sup> found that an AEM with a bulky phosphonium-based cation, tris(2,4,6-trimethoxyphenyl)-polysulfone-methylene quaternary phosphonium hydroxide, maintained its high ionic conductivity for 48 h in 10 M KOH at room temperature and in 1 M KOH at 60 °C.

This approach of monitoring ionic conductivity and IEC under alkaline conditions has provided valuable insights regarding AEM chemical stability. Further insights into chemical stability of the covalently attached cation have also recently been achieved in the literature through the use of proton nuclear magnetic resonance (<sup>1</sup>H NMR) spectroscopy to quantify degradation and identify degradation mechanisms of small molecule ionic salt analogues exposed to alkaline solutions.<sup>9,10,17,30,31</sup> Analogous salts are investigated instead of AEMs because the polymer backbone typically weakens the <sup>1</sup>H NMR signal, making it difficult to determine the mechanism of cation degradation. Additionally, the degraded polymer may no longer be soluble in the same solvent as the undegraded polymer, therefore making degradation analysis via <sup>1</sup>H NMR inaccurate. A few studies have successfully quantified AEM degradation with the use of <sup>1</sup>H NMR spectroscopy;<sup>4,13,21,22,30</sup> conditions for degradation experiments (e.g., temperature, solvent, hydroxide concentration) varied by study such that relative cation stability between studies is difficult to assess. Holdcroft and co-workers<sup>32</sup> found poly[2,2'-(*m*-mesitylene)-5,5'-bis(*N,N'*-dimethylbenzimidazolium)], an AEM that contains its benzimidazolium cation in the polymer backbone, to show no degradation over 10 days in 2 M KOH at 60 °C when monitoring the chemical structure via <sup>1</sup>H NMR. Nuñez and Hickner<sup>13</sup> used <sup>1</sup>H NMR to examine the half-life of BTMA on various backbones, finding it to be particularly stable on a

styrene-based polymer; samples were degraded in hydroxide concentrations polymer; samples were degraded in hydroxide concentrations measured in molar equivalents, a useful technique for comparing studies, and a practice that we have adopted for our current study. Arges and Ramani<sup>21</sup> used two-dimensional NMR correlation spectroscopy to report on the chemical stability of five different cations tethered to a PSF backbone: BTMA, 1,4-dimethylpiperazinium, trimethylphosphonium, 1-methylimidazolium, tris(2,4,6-trimethoxyphenyl)phosphonium. BTMA was more chemically stable than all but 1,4-dimethylpiperazinium, which could potentially be attributed to its lower pK<sub>A</sub> value or steric hindrance effects, while trimethylphosphonium and 1-methylimidazolium degraded rapidly in alkaline media. This technique of comparing several cations on the same backbone within one study is useful, as polymer backbone type may contribute to degradation; thus, changes in backbone from study to study may lead to inconsistencies when comparing cation stability.

In order to more accurately assess cation stability, it is necessary to compare several cation types on the same polymer backbone under the same degradation conditions. While a few additional studies have used this approach,<sup>20,21,30</sup> to date, no studies to our knowledge have quantified the alkaline chemical degradation of AEMs with various covalently linked cation types in tandem with their analogous small molecule ionic salts to definitively determine if there is a correlation. One recent study by Yan and co-workers<sup>30</sup> was successful in using <sup>1</sup>H NMR to quantify the degradation of several pyrrolidinium salts alongside two differently substituted pyrrolidinium-based AEMs and showed the more stable small molecule to also be the more stable polymeric cation. Additional studies attempted a similar approach to examine polymer stability but were unable to draw definitive conclusions for polymeric cation degradation due to commonly faced issues of polymer gelation and H/D exchange.<sup>9,10</sup> The usefulness of past and future small molecule ionic salt degradation studies as tools for predicting relative cation stability in AEMs is dependent upon proof of a correlation between free cation and polymeric cation chemical stability.

In this study, we synthesized polymerized ionic liquids (PILs) containing various covalently attached cations (Scheme 1): butylimidazolium, butylmethylimidazolium, trimethylammonium, pentamethylguanidinium, butylpyrrolidinium, and trimethylphosphonium. The alkaline chemical stabilities of

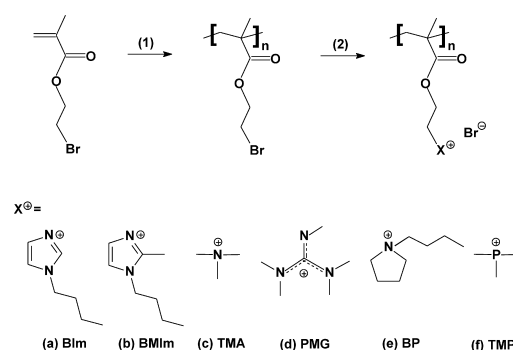
these PILs were investigated and compared to their analogous ionic salts (Scheme 2): 1-butyl-3-methylimidazolium chloride, 1-butyl-2,3-dimethylimidazolium chloride, tetramethylammonium chloride, benzyltrimethylammonium chloride, hexamethylguanidinium chloride, 1,1-butylmethylpyrrolidinium chloride, and tetramethylphosphonium chloride. In order to overcome the aforementioned difficulties in quantifying cation degradation in polymers via  $^1\text{H}$  NMR (e.g., polymer precipitation, weakening of NMR signal by polymer backbone, hydrogen/deuterium exchange), polymers were degraded in  $\text{D}_2\text{O}$  as an alternative to the harsher standard degradation solvent methanol, the PIL chemistry provided high water solubility, such that a significant amount of polymer could be dissolved in  $\text{D}_2\text{O}$  for  $^1\text{H}$  NMR analysis to enable integration, and small amounts of  $\text{H}_2\text{O}$  were used to suppress H/D exchange where necessary. The degradation pathways and extent of chemical stability of the PILs and ionic salts were determined using  $^1\text{H}$  NMR spectroscopy after exposure to 2–20 mol equiv KOH per cation at 30 or 80 °C for 168 h. This tandem study of AEMs alongside analogous small molecule cations establishes whether small molecule studies provide insight into alkaline chemical stability behavior of polymeric cations. Additionally, these results provide a consistent measure of relative alkaline chemical stability of several major cation types.

## EXPERIMENTAL SECTION

**Materials.** *N,N*-Dimethylformamide (DMF, ACS Reagent,  $\geq 99.8\%$ ), 1-butylimidazole (98%), trimethylamine solution (45 wt % in  $\text{H}_2\text{O}$ ), 1-butylpyrrolidine (98%), trimethylphosphine solution (1 M in THF), tetramethylammonium chloride ( $\geq 98\%$ ), benzyltrimethylammonium chloride (97%), tetramethylphosphonium chloride (98%), oxalyl chloride (reagent grade, 98%), ethanol, tetramethylurea, 1,2-dichloroethane (anhydrous, 99.8%), methylamine solution (33 wt % in absolute ethanol), magnesium sulfate (anhydrous, ReagentPlus, 99%), diethyl ether (anhydrous,  $\geq 99.7\%$ , contains 1 ppm BHT inhibitor), hexane (ACS Reagent,  $\geq 98.5\%$ ), tetrahydrofuran (THF,  $\geq 99.9\%$ ), methanol (ACS Reagent,  $\geq 99.8\%$ ), potassium hydroxide (KOH,  $\geq 90\%$ , reagent grade), deuterium oxide ( $\text{D}_2\text{O}$ , 99.98 atom % D), and dimethyl- $d_6$  sulfoxide ( $\text{DMSO-}d_6$ , 99.9 atom % D, contains 0.03% v/v TMS) were used as received from Sigma-Aldrich. 1-Butyl-2-methylimidazole ( $>98\%$ ), 1-butyl-3-methylimidazolium chloride ( $>99\%$ ), 1-butyl-2,3-dimethylimidazolium chloride ( $>99\%$ ), and 1-butyl-1-methylpyrrolidinium chloride (99%) were used as received from Iolitec. Hexamethylguanidinium chloride (98%) was used as received from Fisher Scientific. Azobis(isobutyronitrile) (AIBN, 98%, Sigma-Aldrich) was purified by recrystallization twice from methanol.

**Synthesis of Poly(BrEMA).** Synthesis of the nonionic precursor monomer 2-bromoethyl methacrylate (BrEMA) was performed according to a procedure in the literature.<sup>33</sup> The synthesis of the nonionic precursor homopolymer, poly(BrEMA), was performed using conventional free-radical polymerization as shown in Scheme 3(1). A typical example is given as follows. 5.0 g (25.9 mmol) of BrEMA monomer in DMF (BrEMA/DMF 1/1 w/w) and 22.3 mg (0.129 mmol) of AIBN (BrEMA/AIBN 200/1 mol/mol) were mixed in a 200 mL round-bottom flask and reacted under  $\text{N}_2$  for 2 h at 60 °C. The resulting polymer was precipitated into methanol twice and dried under vacuum in an oven at room temperature for 24 h. Yield: 0.85 g of solid particles (17.0%).  $^1\text{H}$  NMR (500 MHz,  $\text{CDCl}_3$ , 23 °C)  $\delta$  (ppm): 4.47–4.19 (s, 2H, O– $\text{CH}_2$ – $\text{CH}_2$ –Br), 3.66–3.47 (s, 2H, O– $\text{CH}_2$ – $\text{CH}_2$ –Br), 2.12–1.84 (d, 3H,  $\text{CH}_2$ – $\text{C}(\text{CH}_3)$ ), 1.12 (s, 1H,  $\text{HCH}$ – $\text{C}(\text{CH}_3)$ ), 0.98 (s, 1H,  $\text{HCH}$ – $\text{C}(\text{CH}_3)$ ) (NMR, Figure 1). SEC (THF, 40 °C):  $M_n = 59.15 \text{ kg mol}^{-1}$ ,  $M_w/M_n = 1.85$  (against PS standards). Three batches of poly(BrEMA) were synthesized (0.85, 0.83, and 1.13 g with yields of 17.0, 16.6, and 18.8%, respectively) to produce the PILs in this study with similar  $M_n$  and PDIs.

## Scheme 3. Synthesis of PIL Homopolymer, Poly(MEX-Br);<sup>a</sup> X = Various Cations (a–f)



<sup>a</sup>(1) AIBN, DMF, 60 °C, 2 h; (2a) 1-butylimidazole, DMF, 80 °C, 48 h; (2b) 1-butyl-2-methylimidazole, DMF, 80 °C, 48 h; (2c) aqueous trimethylamine, DMF, room temperature, 48 h; (2d) 1,1,2,3,3-pentamethylguanidine (PMG), DMF, room temperature, 24 h; (2e) 1-butylpyrrolidine, DMF, 80 °C, 24 h; (2f) trimethylphosphine/THF solution, DMF, room temperature, 24 h.

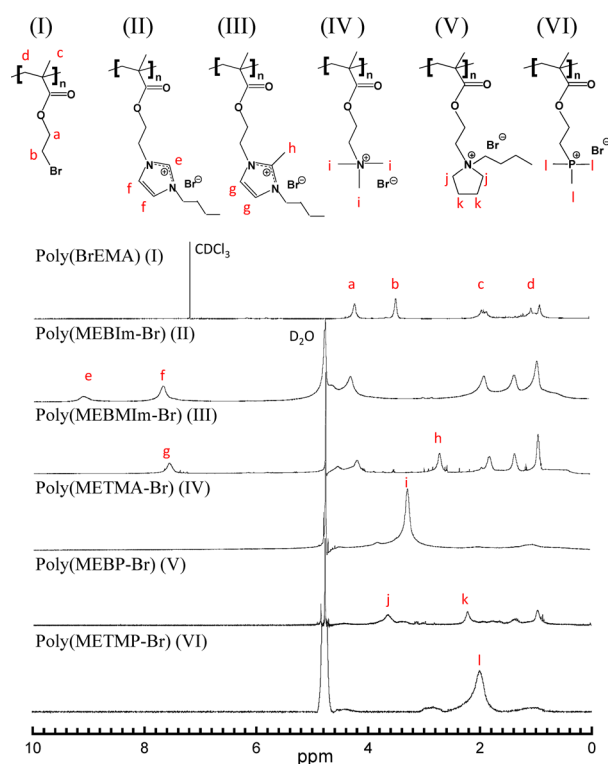


**Figure 1.**  $^1\text{H}$  NMR spectra for (I) poly(BrEMA), (II) poly(MEBIm-Br), (III) poly(MEBMIm-Br), (IV) poly(METMA-Br), (V) poly(MEBP-Br), and (VI) poly(METMP-Br).

**Synthesis of Poly(MEBIm-Br).** Synthesis of the PIL homopolymer, poly(MEBIm-Br) [MEBIm-Br = 1-[(2-methacryloyloxy)ethyl]-3-butylimidazolium bromide], is shown in Scheme 3(2a), i.e., functionalization of nonionic precursor homopolymer, 2-bromoethyl methacrylate, to form an ionic homopolymer. A typical example is given as follows. 0.200 g (1.03 mmol) of poly(BrEMA) was first dissolved in  $\sim 2$  mL of DMF in a 50 mL vial. 0.642 g (5.17 mmol) of 1-butylimidazole (poly(BrEMA)/1-butylimidazole, 1/5 mol/mol) was then mixed into the vial. The solution was stirred at 80 °C for 48 h. The resulting polymer was precipitated twice into hexane and dried under vacuum in an oven at room temperature for 24 h. Yield: 0.267 g (0.841 mmol) of solid particles (81.2%).  $^1\text{H}$  NMR (500 MHz,  $\text{D}_2\text{O}$ , 23 °C)  $\delta$  (ppm): 9.38–8.76 (s, 1H, N– $\text{CH}=\text{N}$ ), 7.98–7.17 (s, 2H,

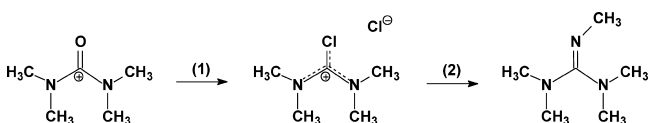
$N-CH=CH-N$ ), 4.54–3.91 (m, 6H,  $N-CH_2-CH_2-O$ ,  $N-CH_2-CH_2-CH_2-CH_3$ ), 1.89 (s, 5H,  $CH_2-C(CH_3)_2$ ,  $N-CH_2-CH_2-CH_2-CH_3$ ), 1.34 (s, 3H,  $N-CH_2-CH_2-CH_2-CH_3$ ,  $HCH-C(CH_3)_3$ ), 0.93 (s, 4H,  $N-CH_2-CH_2-CH_2-CH_3$ ,  $HCH-C(CH_3)_3$ ) (NMR, Figure 1).

**Synthesis of Poly(MEBMIm-Br).** Synthesis of the PIL homopolymer, poly(MEBMIm-Br) [MEBMIm-Br = 1-[(2-methacryloyloxy)ethyl]-3-butylmethylimidazolium bromide], is shown in Scheme 3(2b). A typical example is given as follows. 0.200 g (1.03 mmol) of poly(BrEMA) was first dissolved in ~2 mL of DMF in a 50 mL vial. 0.715 g (5.18 mmol) of 1-butyl-3-methylimidazole (poly(BrEMA)/1-butyl-3-methylimidazole, 1/5 mol/mol) was then mixed into the vial. The solution was stirred at 80 °C for 48 h. The resulting polymer was precipitated twice into hexane and dried under vacuum in an oven at room temperature for 24 h. Yield: 0.261 g (0.788 mmol) of solid particles (76.5%).  $^1H$  NMR (500 MHz,  $D_2O$ , 23 °C)  $\delta$  (ppm): 7.75–7.37 (s, 2H,  $N-CH=CH-N$ ), 4.68–4.01 (m, 6H,  $N-CH_2-CH_2-O$ ,  $N-CH_2-CH_2-CH_2$ ), 3.28–3.58 (s, 3H,  $N-C-CH_3=N$ ), 1.91 (s, 4H,  $CH_2-C(CH_3)_2$ ,  $N-CH_2-CH_2-CH_2-CH_3$ ), 1.35 (s, 3H,  $N-CH_2-CH_2-CH_2-CH_3$ ,  $HCH-C(CH_3)_3$ ), 0.91 (s, 4H,  $N-CH_2-CH_2-CH_2-CH_3$ ,  $HCH-C(CH_3)_3$ ) (NMR, Figure 1).

**Synthesis of Poly(METMA-Br).** Synthesis of the PIL homopolymer, poly(METMA-Br) [METMA-Br = 1-[(2-methacryloyloxy)ethyl]-trimethylammonium bromide], is shown in Scheme 3(2c). A typical example is given as follows. 0.730 g (3.78 mmol) of poly(BrEMA) was first dissolved in ~2 mL of DMF in a 50 mL vial. 1.118 g (18.9 mmol) of trimethylamine in aqueous solution (poly(BrEMA)/trimethylamine, 1/5 mol/mol) was then mixed into the vial. The solution was stirred at room temperature for 48 h. The resulting polymer was precipitated twice into diethyl ether and dried under vacuum in an oven at room temperature for 24 h. Yield: 0.85 g (3.37 mmol) of solid particles (89.2%).  $^1H$  NMR (500 MHz,  $D_2O$ , 23 °C)  $\delta$  (ppm): 4.64–4.25 (s, 2H,  $N-CH_2-CH_2-O$ ), 3.98–3.62 (s, 2H,  $N-CH_2-CH_2-O$ ), 3.64–2.97 (s, 9H,  $N-(CH_3)_3$ ), 2.17–1.86 (s, 3H,  $CH_2-C(CH_3)_2$ ), 1.28–0.81 (s, 2H,  $CH_2-C(CH_3)_2$ ) (NMR, Figure 1).

**Synthesis of 1,1,2,3,3-Pentamethylguanidine (PMG).** To synthesize a PIL homopolymer with pentamethylguanidinium as the cation, 1,1,2,3,3-pentamethylguanidine was first synthesized (Scheme 4). A 250 mL two-necked flask was charged with 50 mL of dry 1,2-

**Scheme 4. Synthesis of 1,1,2,3,3-Pentamethylguanidine (PMG)<sup>a</sup>**



<sup>a</sup>(1) Oxalyl chloride, dichloroethane, 60 °C, 2 h; (2) methylamine/ethanol solution, dropwise, 0 °C, 1 h.

dichloroethane and 4.65 g (40 mmol) of tetramethylurea. Oxalyl chloride (5.65 mL, 64.8 mmol) was added at room temperature, and the solution was heated for 2 h at 60 °C. The solvent was removed under vacuum, the residual yellow solid was dissolved in 20 mL of dry ethanol, and 33.0 g of 33 wt % methylamine in dry ethanol (11.0 g or 354.8 mmol of methylamine) was added dropwise at 0 °C. The reaction mixture was allowed to warm slowly to room temperature, stirred overnight, and then refluxed for 4 h. The solvent was evaporated under vacuum, and the residue was treated with 30% aqueous NaOH. The organic layer was extracted with ether and dried with anhydrous magnesium sulfate, and the solvent was evaporated. Distillation of the residue under reduced pressure at 100 °C yielded 3.22 g (62.3%) of PMG.  $^1H$  NMR (500 MHz,  $CDCl_3$ , 23 °C)  $\delta$  (ppm): 2.90 (s, 3H), 2.80 (s, 6H) and 2.66 (s, 6H) (NMR, Figure S1).

**Synthesis of Poly(MEPMG-Br).** Synthesis of the PIL homopolymer, poly(MEPMG-Br) [MEPMG-Br = 1-[(2-methacryloyloxy)ethyl]-pentamethylguanidinium bromide], is shown in Scheme

3(2d). A typical example is given as follows. 0.400 g (2.07 mmol) of poly(BrEMA) was first dissolved in ~2 mL of DMF in a 50 mL vial. 0.486 g (3.77 mmol) of 1,1,2,3,3-pentamethylguanidine (PMG) (poly(BrEMA)/PMG, 1/2 mol/mol) was then mixed into the vial. The solution was stirred at room temperature for 24 h. The resulting polymer was precipitated twice into diethyl ether and dried under vacuum in an oven at room temperature for 24 h. Yield: 0.53 g (1.708 mmol) of solid particles (82.5%).  $^1H$  NMR (500 MHz,  $DMSO-d_6$ , 23 °C)  $\delta$  (ppm): 3.55–3.19 (s, 12H,  $C-(N-(CH_3)_2)_2$ ) (NMR, Figure S1).

**Synthesis of Poly(MEBP-Br).** Synthesis of the PIL homopolymer, poly(MEBP-Br) [MEBP-Br = 1-[(2-methacryloyloxy)ethyl]-1-butylpyrrolidinium bromide], is shown in Scheme 3(2e). A typical example is given as follows. 0.500 g (2.59 mmol) of poly(BrEMA) was first dissolved in ~2 mL of DMF in a 50 mL vial. 0.989 g (7.77 mmol) of 1-butylpyrrolidine (poly(BrEMA)/1-butylpyrrolidine, 1/3 mol/mol) was then mixed into the vial. The solution was stirred at 80 °C for 24 h. The resulting polymer was precipitated twice into hexane and dried under vacuum in an oven at room temperature for 24 h. Yield: 0.819 g (2.442 mmol) of solid particles (94.3%).  $^1H$  NMR (500 MHz,  $D_2O$ , 23 °C)  $\delta$  (ppm): 4.64–4.18 (s, 2H,  $N-CH_2-CH_2-O$ ), 3.90–3.45 (s, 6H,  $N-CH_2-CH_2-CH_2-CH_2-N$ ,  $N-CH_2-CH_2-O$ ), 2.35–2.02 (s, 4H,  $N-CH_2-CH_2-CH_2-CH_2-N$ ), 1.51–1.27 (s, 7H,  $N-CH_2-CH_2-CH_2-CH_2-CH_3$ ,  $CH_2-C(CH_3)_2$ ), 1.08–0.80 (s, 5H,  $N-CH_2-CH_2-CH_2-CH_2-CH_3$ ,  $CH_2-C(CH_3)_2$ ) (NMR, Figure 1).

**Synthesis of Poly(METMP-Br).** Synthesis of the PIL homopolymer, poly(METMP-Br) [METMP-Br = 1-[(2-methacryloyloxy)ethyl]-trimethylphosphonium bromide], is shown in Scheme 3(2f). A typical example is given as follows. 0.500 g (2.59 mmol) of poly(BrEMA) was first dissolved in ~2 mL of DMF in a 50 mL vial. 0.591 g (7.77 mmol) of trimethylphosphine in THF solution (poly(BrEMA)/trimethylphosphine, 1/3 mol/mol) was then mixed into the vial. The solution was stirred at room temperature for 24 h. The resulting polymer was precipitated twice into diethyl ether and dried under vacuum in an oven at room temperature for 24 h. Yield: 0.467 g (1.735 mmol) of solid particles (67.0%).  $^1H$  NMR (500 MHz,  $D_2O$ , 23 °C)  $\delta$  (ppm): 4.55–4.14 (s, 2H,  $P-CH_2-CH_2-O$ ), 3.93–3.50 (s, 2H,  $P-CH_2-CH_2-O$ ), 2.50–1.62 (s, 9H,  $P-(CH_3)_3$ ), 1.44–0.61 (s, 5H,  $CH_2-C(CH_3)_2$ ) (NMR, Figure 1).

**Characterization.** All chemical structures of the PIL homopolymers were characterized by  $^1H$  NMR spectroscopy using a Varian 500 MHz spectrometer at 23 °C with  $D_2O$  as the solvent. The chemical shifts were referenced to water at 4.75 ppm. Chemical structures of poly(BrEMA) and PMG were also characterized by  $^1H$  NMR spectroscopy and referenced to  $CDCl_3$  at 7.27 ppm. The molecular weights and molecular weight distributions of precursor PIL homopolymer were determined by size exclusion chromatography (SEC) using a Waters GPC system equipped with a THF Styragel column (Styragel@HR SE, effective separation of molecular weight range: 2–4000  $kg\ mol^{-1}$ ) and a 2414 reflective index (RI) detector. All measurements were performed at 40 °C. THF was used as the mobile phase at a flow rate of 1.0 mL/min. PS standards (Shodex, Japan) with molecular weights ranging from 2.97 to 983  $kg\ mol^{-1}$  were used for calibration.

**Alkaline Chemical Stability Analysis.** The chemical stability of ionic salts and PIL homopolymers was examined using  $^1H$  NMR spectroscopy with  $D_2O$  as the solvent. The stability study was performed under alkaline conditions in NMR tubes. Ionic salts (25.0 mg) were exposed to different KOH concentrations (2, 20, and 50 mol equiv) in 1 mL of  $D_2O$  at 30 or 80 °C for 168 h, followed by  $^1H$  NMR experiments to quantify chemical degradation. PIL homopolymers (8.0 mg) dissolved in 1 mL of  $D_2O$  were exposed to 2 and 20 equiv KOH at 30 or 80 °C for 168 h, followed by  $^1H$  NMR experiments. Note that all KOH concentrations are in excess of 1 equiv to ensure full ion exchange of ionic salts and PILs.

## RESULTS AND DISCUSSION

**Ionic Salt Alkaline Chemical Stability.** In order to investigate the alkaline stability of PILs with covalently tethered

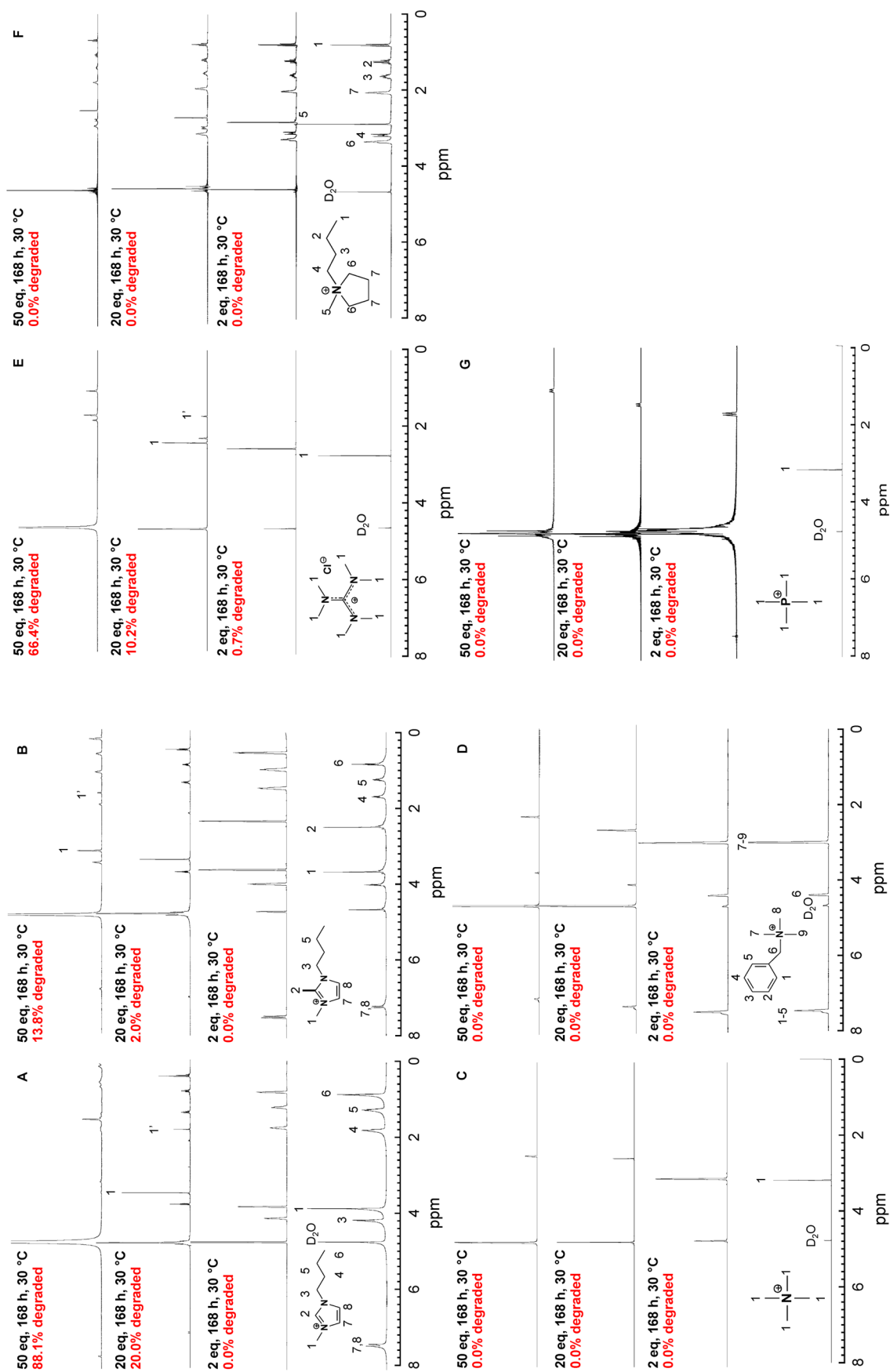
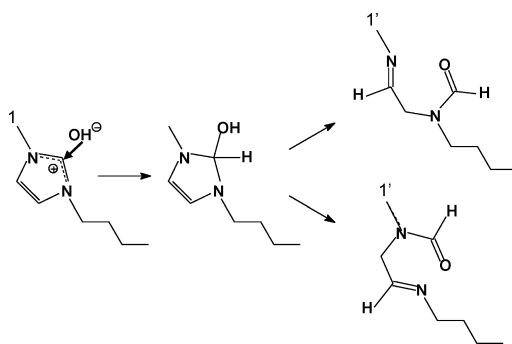


Figure 2. <sup>1</sup>H NMR spectra for (A) BMIm<sup>+</sup>Cl<sup>-</sup>, (B) BDMIm<sup>+</sup>Cl<sup>-</sup>, (C) TMA<sup>+</sup>Cl<sup>-</sup>, (D) BTMA<sup>+</sup>Cl<sup>-</sup>, (E) HMG<sup>+</sup>Cl<sup>-</sup>, (F) BMP<sup>+</sup>Cl<sup>-</sup>, (G) TMP<sup>+</sup>Cl<sup>-</sup> in 2, 20, and 50 equiv KOH/D<sub>2</sub>O at 30 °C for 168 h.

cations, the analogous small molecule model compounds were first studied: 1-butyl-3-methylimidazolium chloride (BMIm<sup>+</sup>Cl<sup>-</sup>), 1-butyl-2,3-dimethylimidazolium chloride (BDMIm<sup>+</sup>Cl<sup>-</sup>), tetramethylammonium chloride (TMA<sup>+</sup>Cl<sup>-</sup>), benzyltrimethylammonium chloride (BTMA<sup>+</sup>Cl<sup>-</sup>), hexamethylguanidinium chloride (HMG<sup>+</sup>Cl<sup>-</sup>), 1,1-butylmethylpyrrolidinium chloride (BMP<sup>+</sup>Cl<sup>-</sup>), and tetramethylphosphonium chloride (TMP<sup>+</sup>Cl<sup>-</sup>) (Scheme 2). The purity and chemical structure of these ionic salts were confirmed by <sup>1</sup>H NMR prior to alkaline chemical stability experiments (Figure 2).

The degradation of the ionic salts was quantified by <sup>1</sup>H NMR spectroscopy, where the effects of alkaline concentration and reaction temperature on the alkaline chemical stability of the cations were investigated. Figure 2 shows <sup>1</sup>H NMR spectra of each ionic salt after 1 week (168 h) exposure to 2, 20, and 50 equiv KOH/D<sub>2</sub>O solutions at 30 °C. In Figure 2A, the <sup>1</sup>H NMR spectra of BMIm<sup>+</sup>Cl<sup>-</sup> shows no degradation upon exposure to 2 equiv, while exposure to 20 and 50 equiv shows a new peak at ~1.8 ppm (labeled 1'), where this peak can be attributed to a ring-opening reaction as described in the literature.<sup>4</sup> Scheme 5 shows the ring-opening degradation

**Scheme 5. Ring-Opening Reaction of 3-Butyl-1-methylimidazolium**



mechanism for BMIm<sup>+</sup>Cl<sup>-</sup> in alkaline media, where the new peak is attributed to the proton at position 1'. The degree of degradation by this ring-opening reaction was calculated by the relative integrations of the indicated <sup>1</sup>H resonances (i.e., 1'/(1 + 1')), Scheme 5) and was calculated to be 20.0% and 88.1% for BMIm<sup>+</sup>Cl<sup>-</sup> in 20 and 50 equiv KOH/D<sub>2</sub>O solutions, respectively, at 30 °C for 168 h. Similarly, a ring-opening reaction was observed in the C2-methyl-substituted imidazolium salt (Figure 2B), BDMIm<sup>+</sup>Cl<sup>-</sup>; the degree of degradation at 30 °C for 168 h was found to be 0.0, 2.0, and 13.8% in 2, 20, and 50 equiv KOH/D<sub>2</sub>O solutions, respectively, indicating that methyl substitution in the C2 position of imidazolium salts hinders hydroxide attack compared to the C2-unsubstituted ionic salt (BMIm<sup>+</sup>Cl<sup>-</sup>). These results corroborate with recent findings in the literature.<sup>9</sup> It is also notable that in both salts the proton peaks associated with the C2, C4, and C5 positions of imidazole rings disappear in the presence of D<sub>2</sub>O due to the hydrogen/deuterium (H/D) exchange reaction.

Figure 3 shows <sup>1</sup>H NMR spectra of each ionic salt in this study after 168 h exposure to 2 and 20 equiv KOH/D<sub>2</sub>O solutions at a higher temperature (80 °C). Degradation is accelerated by increased temperature, as seen in Figure 3A,B, where at 80 °C both imidazolium salts show earlier signs of ring-opening reactions with 0.5% degradation for 2 equiv compared with 0.0% at 30 °C at this KOH concentration. For

20 equiv and 80 °C, degradation is further increased to 98.7% and 7.5% (compared with 20.0% and 2.0% at 30 °C) for BMIm<sup>+</sup>Cl<sup>-</sup> and BDMIm<sup>+</sup>Cl<sup>-</sup>, respectively. BDMIm<sup>+</sup>Cl<sup>-</sup> appears to be the more chemically stable imidazolium salt at high temperature as well as low temperature.

Figures 2C,D and 3C,D show <sup>1</sup>H NMR spectra for ammonium-based ionic salts, TMA<sup>+</sup>Cl<sup>-</sup> and BTMA<sup>+</sup>Cl<sup>-</sup>, after 168 h exposure to KOH/D<sub>2</sub>O at 30 and 80 °C, respectively. Though cation peaks do shift as expected after addition of hydroxide, no other changes were observed as the original cation peaks are still present and no new peaks appear under any measured conditions, indicating high alkaline stability in up to at least 50 equiv KOH/D<sub>2</sub>O at 30 °C and 20 equiv KOH/D<sub>2</sub>O at 80 °C. It is possible to show chemical degradation of ammonium salts via nucleophilic attack at higher temperatures or with other solvents (e.g., methanol);<sup>24</sup> however, for consistency within this study, the ionic salts were degraded under the same conditions as the PILs, which were degraded in the conditions most applicable to a fuel cell (e.g., water, 80 °C), which would also not cause precipitation of the degraded polymer. The phosphonium analogue to TMA<sup>+</sup>Cl<sup>-</sup>, TMP<sup>+</sup>Cl<sup>-</sup> (Figures 2G and 3G), likewise shows no chemical degradation after 168 h under similar measured conditions: 2, 20, and 50 equiv KOH/D<sub>2</sub>O at 30 °C; 2 and 20 equiv KOH/D<sub>2</sub>O at 80 °C.

Figures 2E and 3E show <sup>1</sup>H NMR spectra for guanidinium ionic salt, HMG<sup>+</sup>Cl<sup>-</sup>, after 168 h exposure to KOH/D<sub>2</sub>O at 30 and 80 °C, respectively. As observed for the imidazolium salts, degradation increased with increasing hydroxide concentration as well as increasing temperature. In Figure 2E, new peaks observed at ~1.8 ppm (labeled 1') were attributed to a nucleophilic substitution reaction as described in the literature.<sup>28</sup> Scheme 6 shows the S<sub>N</sub>2 degradation of HMG<sup>+</sup>Cl<sup>-</sup> in alkaline media, where the new peak was attributed to the protons at position 1'. The degree of degradation was determined by the relative integrations of <sup>1</sup>H resonances of the degraded and nondegraded cation (i.e., 2(1')/(3(1) + 2(1')), Scheme 6) and was found to be 0.7, 10.2, and 66.4% in 2, 20, and 50 equiv KOH/D<sub>2</sub>O solutions, respectively, at 30 °C for 168 h. Figure 3E shows that as temperature increased to 80 °C, degradation increased to 60.9% and 100% for 2 and 20 equiv, respectively.

Similar to results for ammonium and phosphonium salts, the pyrrolidinium salt BMP<sup>+</sup>Cl<sup>-</sup> in Figures 2F and 3F shows no chemical degradation in alkaline media. This is an interesting result, as other ring structures (imidazolium salts) show quantifiable degradation by ring-opening reaction under the same conditions. One potential explanation for improved chemical stability is increased resistance to bond breakage due to lack of polarizability in the resonance-free ring structure of a pyrrolidinium versus the conjugated bonds of the imidazolium ring; steric hindrance as a result of the butyl and methyl substituents in the N1 position may also be providing protection from hydroxide attack.

Overall, high alkaline chemical stability was observed in the ammonium, phosphonium, and pyrrolidinium ionic salts, TMA<sup>+</sup>Cl<sup>-</sup>, BTMA<sup>+</sup>Cl<sup>-</sup>, TMP<sup>+</sup>Cl<sup>-</sup>, and BMP<sup>+</sup>Cl<sup>-</sup>, as no quantifiable degradation was evidenced inasmuch as 50 equiv KOH/D<sub>2</sub>O at 30 °C and 20 equiv KOH/D<sub>2</sub>O at 80 °C. Of the remaining salts, the C2-methyl substituted imidazolium, BDMIm<sup>+</sup>Cl<sup>-</sup>, was observed to be the most chemically stable, with 7.5% degradation at 20 equiv KOH/D<sub>2</sub>O at 80 °C, compared with 98.7% and 100% degradation for BMIm<sup>+</sup>Cl<sup>-</sup>

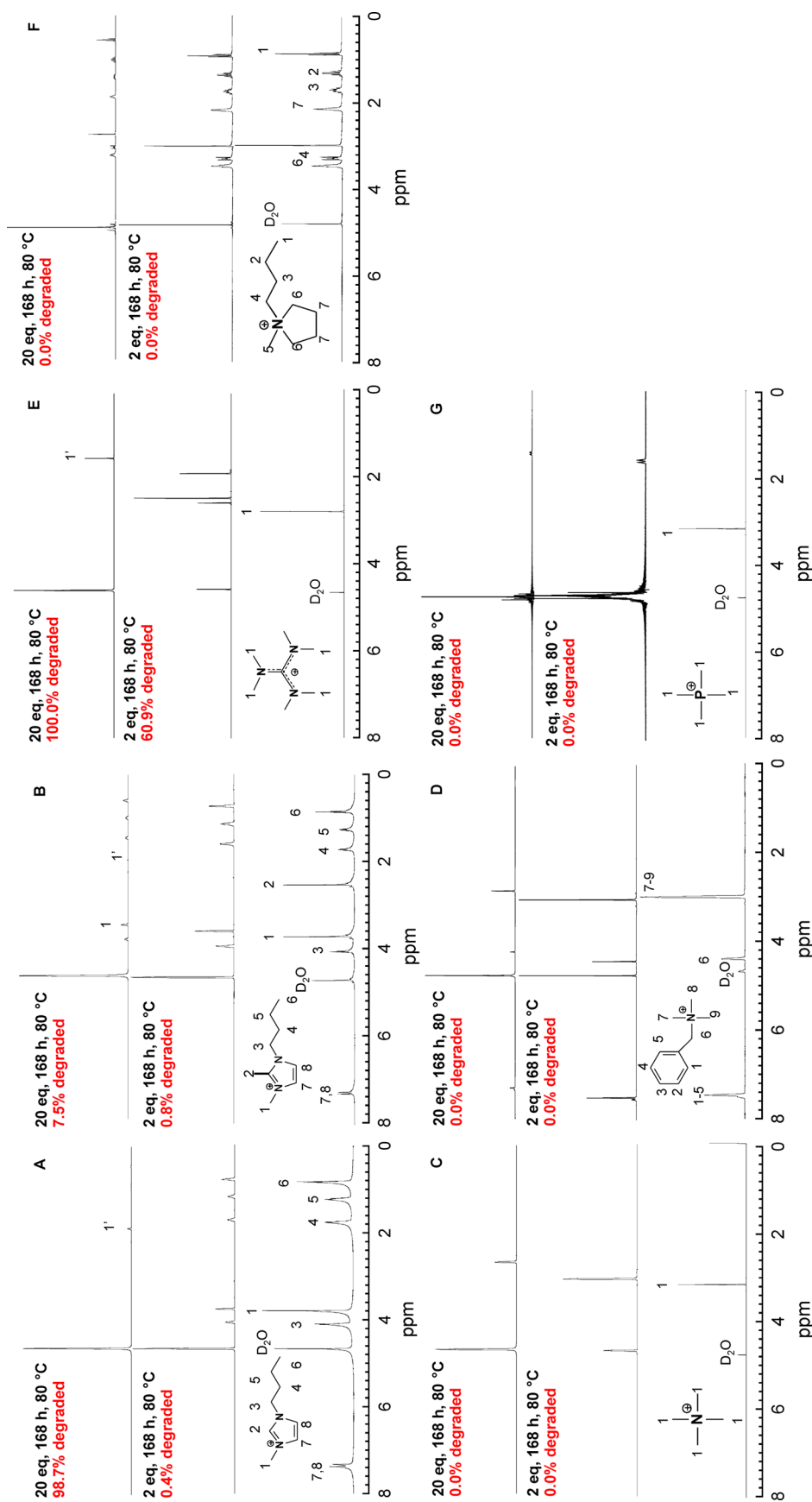
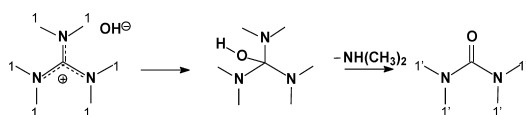


Figure 3.  $^1\text{H}$  NMR spectra for (A)  $\text{BMIm}^+\text{Cl}^-$ , (B)  $\text{BDMIm}^+\text{Cl}^-$ , (C)  $\text{TMA}^+\text{Cl}^-$ , (D)  $\text{BTMA}^+\text{Cl}^-$ , (E)  $\text{HMG}^+\text{Cl}^-$ , (F)  $\text{BMP}^+\text{Cl}^-$ , and (G)  $\text{TMP}^+\text{Cl}^-$  in 2 and 20 equiv  $\text{KOH}/\text{D}_2\text{O}$  at 80 °C for 168 h.

### Scheme 6. Nucleophilic Substitution Reaction of Hexamethylguanidinium



and  $\text{HMG}^+\text{Cl}^-$ , respectively, under the same conditions. A summary of the alkaline chemical degradation results for the small molecule ionic salts is listed in Table 1.

**PIL Alkaline Chemical Stability.** We synthesized and investigated the chemical stability of methacrylate-based PILs consisting of various covalently attached cations: butylimidazolium, butylmethylimidazolium, trimethylammonium, pentamethylguanidinium, butylpyrrolidinium, and trimethylphosphonium. These cations are analogous to the ionic salts in this study. The purity, chemical structure, and degree of functionalization of these PILs were confirmed by  $^1\text{H}$  NMR prior to alkaline chemical stability experiments (see Figure 1). PIL cation degradation was also quantified by  $^1\text{H}$  NMR spectroscopy, where the effects of alkaline concentration and

reaction temperature on the alkaline chemical stability of the covalently tethered cations were investigated.

Figures 4 and 5 show  $^1\text{H}$  NMR spectra of each PIL after 168 h exposure to 2 and 20 equiv  $\text{KOH}/\text{D}_2\text{O}$  solutions at 30 and 80  $^\circ\text{C}$ , respectively. In Figure 4A, the  $^1\text{H}$  NMR spectra of poly(MEBIm-Br) show two new peaks at  $\sim 7.5$  and  $\sim 8.43$  ppm (labeled  $f'$  and  $e'$ , respectively), where these peaks are attributed to ring-opening degradation as seen in the analogous small molecule salt and described in the literature.<sup>4</sup> Likewise, in Figure 4B, two new peaks appear at  $\sim 7.48$  and  $\sim 8.42$  ppm (labeled  $h'$  and  $g'$ , respectively) in the  $^1\text{H}$  NMR spectra of poly(MEBMIm-Br), also indicating a ring-opening mechanism. Alkaline degradation by this ring-opening reaction was calculated by the relative integrations of the indicated  $^1\text{H}$  resonances (i.e.,  $f'/(f + f')$  for poly(MEBIm-Br) and  $g'/(g + g')$  for poly(MEBMIm-Br); degradation mechanism shown in Scheme 7) and was calculated as 12.1 and 22.3% for poly(MEBIm-Br) and 15.5 and 23.9% for poly(MEBMIm-Br) at 2 and 20 equiv, respectively, at 30  $^\circ\text{C}$  for 168 h. Figure 5A,B shows the same new peaks arising under high temperature conditions; the extent of degradation was calculated as 19.4 and 33.5% for poly(MEBIm-Br) and 31.3 and 38.2% for poly-

**Table 1. Alkaline Chemical Degradation Results for Ionic Salts**

ionic salt	temp ( $^\circ\text{C}$ )	KOH conc (mol equiv)	KOH conc (M)	NMR spectrum	degradation <sup>a</sup> (%)	degradation pathway
BMIm <sup>+</sup> Cl <sup>-</sup>	30	2	0.29	Figure 2A	0.0	Scheme 5
	30	20	2.86	Figure 2A	20.0	
	30	50	7.16	Figure 2A	88.1	
	80	2	0.29	Figure 3A	0.4	
	80	20	2.86	Figure 3A	98.7	
BDMIm <sup>+</sup> Cl <sup>-</sup>	30	2	0.27	Figure 2B	0.0	Scheme 5 <sup>b</sup>
	30	20	2.65	Figure 2B	2.0	
	30	50	6.63	Figure 2B	13.8	
	80	2	0.27	Figure 3B	0.8	
	80	20	2.65	Figure 3B	7.5	
TMA <sup>+</sup> Cl <sup>-</sup>	30	2	0.46	Figure 2C	0	
	30	20	4.56	Figure 2C	0	
	30	50	11.41	Figure 2C	0	
	80	2	0.46	Figure 3C	0	
	80	20	4.56	Figure 3C	0	
BTMA <sup>+</sup> Cl <sup>-</sup>	30	2	0.27	Figure 2D	0	
	30	20	2.69	Figure 2D	0	
	30	50	6.74	Figure 2D	0	
	80	2	0.27	Figure 3D	0	
	80	20	2.69	Figure 3D	0	
HMG <sup>+</sup> Cl <sup>-</sup>	30	2	0.29	Figure 2E	0.7	Scheme 6
	30	20	2.86	Figure 2E	10.2	
	30	50	7.16	Figure 2E	66.4	
	80	2	0.29	Figure 3E	60.9	
	80	20	2.86	Figure 3E	100	
BMP <sup>+</sup> Cl <sup>-</sup>	30	2	0.28	Figure 2F	0	
	30	20	2.81	Figure 2F	0	
	30	50	7.03	Figure 2F	0	
	80	2	0.28	Figure 3F	0	
	80	20	2.81	Figure 3F	0	
TMP <sup>+</sup> Cl <sup>-</sup>	30	2	0.39	Figure 2G	0	
	30	20	3.89	Figure 2G	0	
	30	50	9.72	Figure 2G	0	
	80	2	0.39	Figure 3G	0	
	80	20	3.89	Figure 3G	0	

<sup>a</sup>All samples were degraded for 168 h. <sup>b</sup>Analogous to degradation pathway of similar ionic salt.

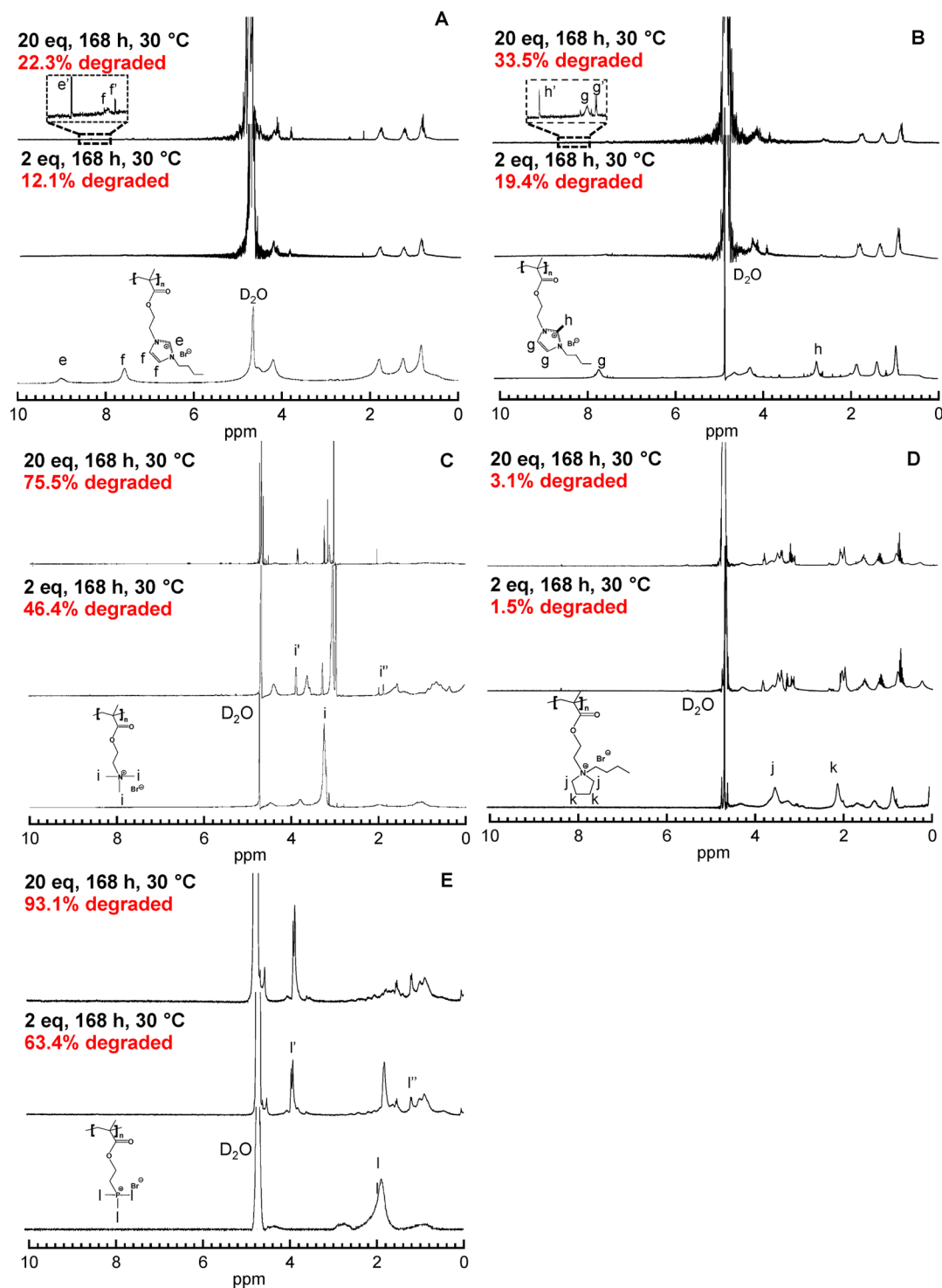


**Figure 4.**  $^1\text{H}$  NMR spectra for (A) poly(MEBIm-Br), (B) poly(MEBMIm-Br), (C) poly(METMA-Br), (D) poly(MEBP-Br), and (E) poly(METMP-Br) in 2 and 20 equiv KOH/ $\text{D}_2\text{O}$  at 30 °C for 168 h.

(MEBMIm-Br) at 2 and 20 equiv, respectively, at 80 °C for 168 h. In contrast to the ionic salt chemical stability results, the C2-methyl-substituted cation showed slightly higher degradation at each condition compared to the unsubstituted cation, indicating that the resistance to ring-opening mechanism provided by steric hindrance of additional moieties in the C2 position that has been seen in the small molecule studies may not translate to covalently tethered cations. It should be noted that for both imidazolium polymers in KOH/ $\text{D}_2\text{O}$  solution the proton peaks

associated with the C2, C4, and C5 positions of imidazole rings diminished more rapidly than could be attributed solely to ring-opening degradation due to an accompanying hydrogen/deuterium (H/D) exchange reaction. It has been shown in previous studies that it is possible to suppress this H/D exchange in order to accurately calculate cation degradation by including 10 wt %  $\text{H}_2\text{O}$  (relative to mass of polymer).<sup>4</sup> Therefore, for the imidazolium PILs only, 80 mg of  $\text{D}_2\text{O}$  was replaced with 80 mg of  $\text{H}_2\text{O}$ , to maintain a total of 1 mL water

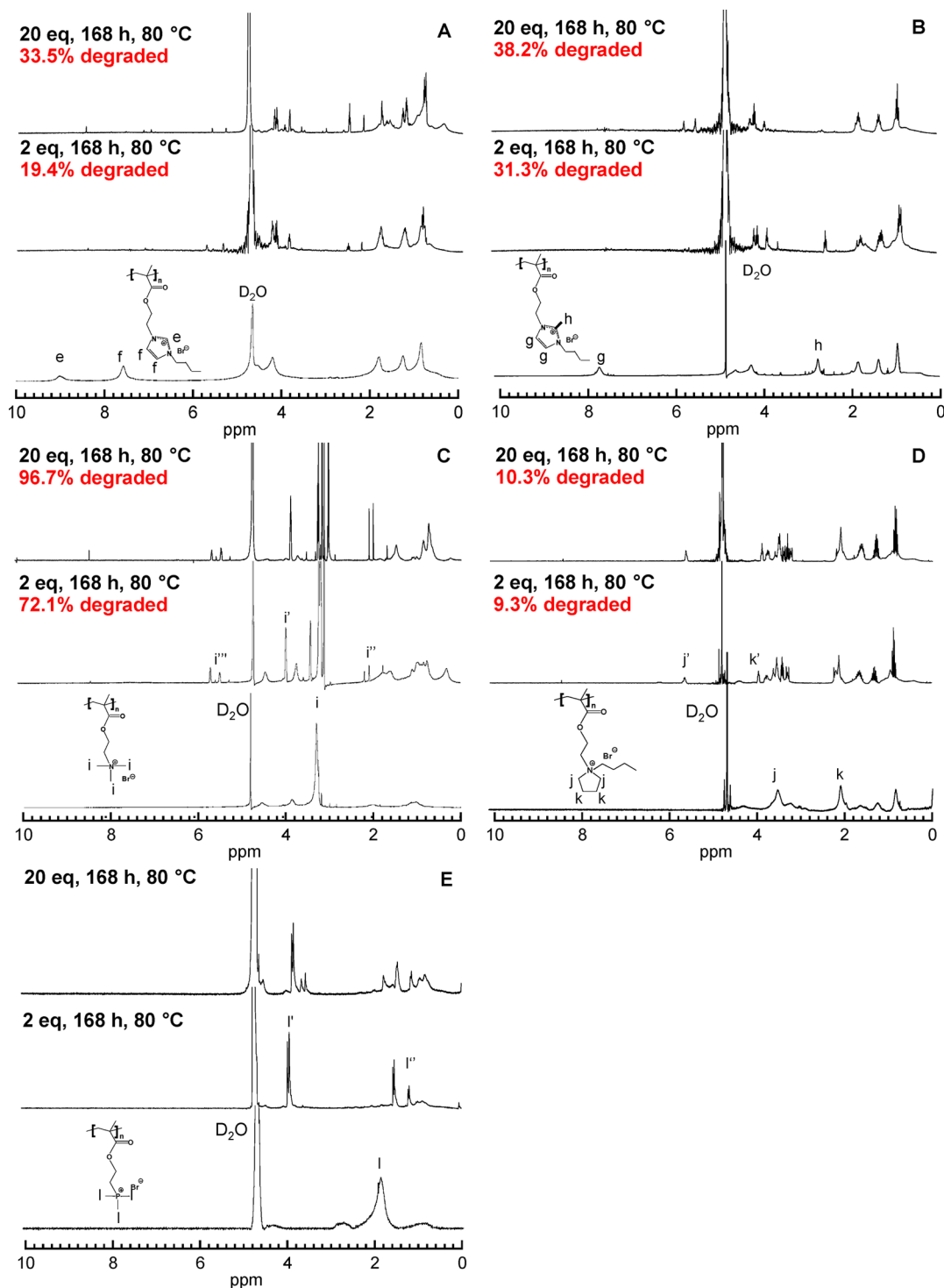


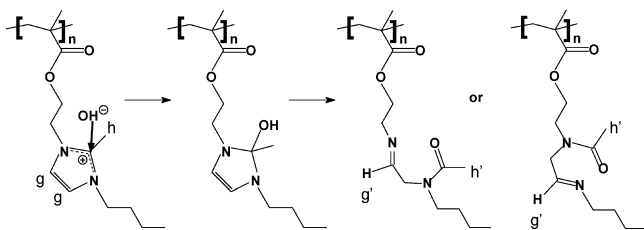
**Figure 5.**  $^1\text{H}$  NMR spectra for (A) poly(MEBIm-Br), (B) poly(MEBMIm-Br), (C) poly(METMA-Br), (D) poly(MEBP-Br) and (E) poly(METMP-Br) in 2 and 20 equiv KOH/ $\text{D}_2\text{O}$  at  $80^\circ\text{C}$  for 168 h.

(deuterated and nondeuterated), while also preventing H/D exchange. Additional  $^1\text{H}$  NMR spectra (Supporting Information Figures S2 and S3) confirm that the exchange is fully suppressed for the imidazolium PILs when  $\text{H}_2\text{O}$  is included. For the remaining three PILs,  $^1\text{H}$  NMR spectra (Figures S4 and S5) confirm that as anticipated, there is no H/D exchange in  $\text{D}_2\text{O}$  at  $80^\circ\text{C}$  for 168 h, such that any reduction in the cation peaks in the presence of KOH can be attributed solely to alkaline degradation reaction; it is therefore not necessary to

include  $\text{H}_2\text{O}$  in the solution. It was also confirmed (Figure S6) that including  $\text{H}_2\text{O}$  would not change the results for these PILs, and thus the imidazolium results in KOH/ $\text{D}_2\text{O}$ / $\text{H}_2\text{O}$  solutions are analogous to results for the other three PILs in KOH/ $\text{D}_2\text{O}$  solutions. Similar results were obtained for the imidazolium salts, where no difference in degradation was observed between  $\text{D}_2\text{O}$  or  $\text{H}_2\text{O}$  solutions (Figure S7).

Figures 4C and 5C show  $^1\text{H}$  NMR spectra for the quaternary ammonium-based PIL, poly(METMA-Br), after 168 h exposure

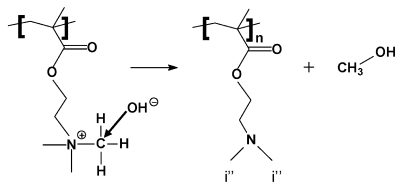
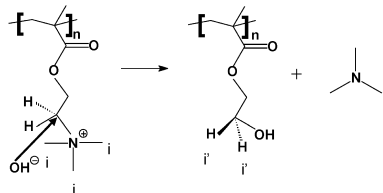
## Scheme 7. Ring-Opening Reaction of Poly(MEBMIm-Br)



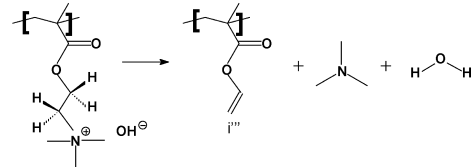
to KOH/D<sub>2</sub>O at 30 and 80 °C, respectively. Two major degradation reactions are generally accepted for pendant quaternary ammonium cations: (1) nucleophilic substitution (S<sub>N</sub>2 reaction) via hydroxide attack on the α carbons resulting in amine and alcohol byproducts and (2) Hofmann degradation (E2 elimination) from the removal of the β hydrogen by hydroxide, resulting in amine and alkene byproducts (Scheme 8).<sup>34</sup> The S<sub>N</sub>2 reaction and E2 elimination occur simulta-

## Scheme 8. Degradation Reactions of Poly(METMA-Br)

Nucleophilic substitution:



Hofmann elimination:

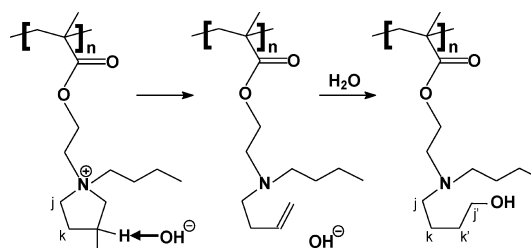


neously, leading to a mixture of byproducts; one mechanism may be preferential depending upon the chemical structure and degradation conditions. In Figure 4C, nucleophilic substitution reactions were observed for the trimethylammonium cation as new peaks appeared at ~3.92 ppm (labeled i') and ~2.09 ppm (labeled i'') in solutions of 2 and 20 equiv KOH/D<sub>2</sub>O at 30 °C; Hofmann elimination reaction was not observed at 30 °C. Extent of degradation of the cation, defined as the relative integrated intensities of corresponding <sup>1</sup>H NMR peaks (i.e., (9i' + 3i'')/(2i + 9i' + 3i'')), was 46.4 and 75.5% for 2 or 20 equiv, respectively, at 30 °C. At 80 °C, in addition to the degradation peaks seen in Figure 4C, Figure 5C shows two additional peaks located at ~5.45 and ~5.67 ppm (labeled i'''). These new peaks indicate degradation by Hofmann elimination occurred at this higher temperature condition; subsequently, relative integration ratios include the new peaks (i.e., (9i' + 3i'' + 9i''')/(2i + 9i' + 3i'' + 9i''')). Cation degradation was quantified as 72.1 and 94.8% upon exposure to 2 and 20 equiv KOH/D<sub>2</sub>O solutions, respectively, at 80 °C. While degradation increased with increasing temperature, the S<sub>N</sub>2 reaction, specifically the

pathway that resulted in a pendant hydroxyl and an amine byproduct, was the primary degradation mechanism at both low and high temperatures.

The guanidinium-based PIL, poly(MEPMG-Br), was not water-soluble and was therefore excluded from the chemical stability study. For the pyrrolidinium-based PIL, poly(MEBP-Br), in Figures 4D and 5D, limited degradation was observed in the <sup>1</sup>H NMR spectra after 168 h exposure to 2 or 20 equiv KOH/D<sub>2</sub>O at 30 and 80 °C, respectively, as a new peak arises at ~5.60 ppm (labeled j'). Similar degradation has been described in the literature; the proposed Hofmann elimination mechanism is shown in Scheme 9.<sup>30</sup> The degree of degradation

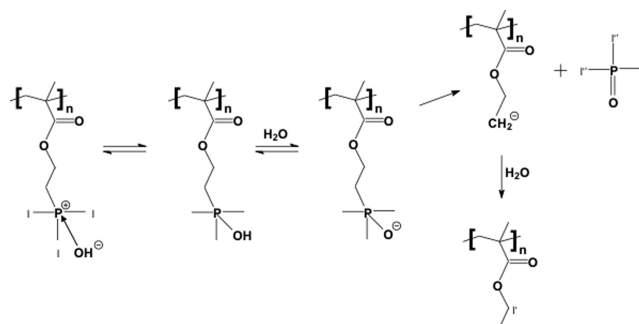
## Scheme 9. Hofmann Elimination Reaction of Poly(MEBP-Br)



of the cation can be calculated by the relative integrated intensities of corresponding <sup>1</sup>H NMR peaks (i.e., j'/(k + j')) and was 9.3 and 10.3% for 2 and 20 equiv, respectively, at 80 °C, indicating a high alkaline chemical stability at these conditions. The Hofmann elimination reaction was further confirmed by the minimal degradation at 30 °C (1.5 and 3.1% for 2 and 20 equiv, respectively), as this mechanism is known to favor higher temperatures.

Figures 4E and 5E show <sup>1</sup>H NMR spectra for the quaternary phosphonium-based PIL, poly(METMP-Br), at 30 and 80 °C, respectively, after 168 h exposure to 2 and 20 equiv KOH/D<sub>2</sub>O solutions. The phosphonium cation is known to degrade by the Cahours–Hofmann reaction, where hydroxide attacks the phosphonium tetrahedron, resulting in phosphine oxide and an alkyl group as byproducts (Scheme 10).<sup>35,36</sup> In both Figures

## Scheme 10. Cahours–Hofmann Reaction of Poly(METMP-Br)



4E and 5E, the two new peaks appearing at ~3.84 and ~3.77 ppm (labeled l') are associated with the –CH<sub>2</sub>– of the alkyl chain remaining on the polymer after the phosphonium group has been cleaved, while the new peak at ~1.12 ppm (labeled l'') is associated with the small molecule byproduct, trimethylphosphonium oxide. Integration of the degradation peaks relative to the remaining covalently tethered polymer cation

Table 2. Alkaline Chemical Degradation Results for PILs with Various Cations

PIL	temp (°C)	KOH conc <sup>a</sup> (mol equiv)	KOH conc (M)	NMR spectrum	cation degradation <sup>b</sup> (%)	degradation pathway
poly(MEBIm-Br)	30	2	0.05	Figure 4A	12.1	Scheme 7 <sup>c</sup>
	30	20	0.50	Figure 4A	22.3	
	80	2	0.05	Figure 5A	19.4	
	80	20	0.50	Figure 5A	33.5	
poly(MEBMIm-Br)	30	2	0.05	Figure 4B	15.5	Scheme 7
	30	20	0.48	Figure 4B	23.9	
	80	2	0.05	Figure 5B	31.3	
	80	20	0.48	Figure 5B	38.2	
poly(METMA-Br)	30	2	0.06	Figure 4C	46.4	Scheme 8
	30	20	0.63	Figure 4C	75.5	
	80	2	0.06	Figure 5C	72.1	
	80	20	0.63	Figure 5C	94.8	
poly(MEBP-Br)	30	2	0.05	Figure 4D	1.5	Scheme 9
	30	20	0.50	Figure 4D	3.1	
	80	2	0.05	Figure 5D	9.3	
	80	20	0.50	Figure 5D	10.3	
poly(METMP-Br)	30	2	0.06	Figure 4E	63.4	Scheme 10
	30	20	0.59	Figure 4E	93.1	
	80	2	0.06	Figure 5E	<i>d</i>	
	80	20	0.59	Figure 5E	<i>d</i>	

<sup>a</sup>In samples of poly(MEBIm-Br) and poly(MEBMIm-Br), 80 mg of D<sub>2</sub>O was replaced with 80 mg of H<sub>2</sub>O to suppress H/D exchange. <sup>b</sup>All samples were degraded for 168 h; amounts refer to both cleaved and uncleaved cation; see Supporting Information for backbone degradation due to hydrolysis. <sup>c</sup>Degradation pathway of poly(MEBIm-Br) is analogous to degradation pathway of poly(MEBMIm-Br). <sup>d</sup>Polymer precipitated under these conditions.

peak (i.e.,  $9I'/(1 + 9I')$ ) yields degradation degrees of 63.4 and 93.1% for 2 or 20 equiv, respectively, at 30 °C. At 80 °C, degradation could not be quantified because the polymer precipitated from solution and the precipitate was black in color. A summary of the alkaline chemical degradation results for the PILs with various cations are listed in Table 2.

Note that in addition to the chemical stability of cations, another potential concern is hydrolysis degradation of the carboxylate ester linkage of the methacrylate-based PIL backbone under alkaline conditions. Although the hydrolysis of a polymeric ester has been reported in the literature, it typically occurs at a much slower rate compared to small molecule esters;<sup>37</sup> degradation rate is significantly dependent on the structure of the polymer backbone, with the hydrolysis of a methacrylate-based polymer observed to occur at a significantly slower rate compared to the acrylate analogue.<sup>38</sup> For poly(methyl methacrylate) (PMMA), studies have confirmed that ~9% of the monomer units are susceptible to hydrolysis.<sup>38</sup> Previous research has suggested ester hydrolysis of the hydroxide-exchanged methacrylate-based PIL, poly(MEBIm-OH), occurs after the ring-opening mechanism of the butylimidazolium cation, as ring-opened imidazolium byproducts were present in both covalently attached (non-hydrolyzed) and cleaved (hydrolyzed) forms; ~30% of the ring-opened byproducts (~11% of the total monomer units) were cleaved from the polymer via ester hydrolysis after 168 h at 80 °C and 1 M KOH.<sup>4</sup> In this study, for the imidazolium-based PILs, poly(MEBIm-Br) and poly(MEBMIm-Br), ~18% and ~15% of the total monomer units (~55% and ~40% of the ring-opened byproducts), respectively, had cleaved from the polymer after 168 h at 80 °C and 20 equiv KOH (see Figure S8, Schemes S1 and S2); these results are in relatively good agreement with results for PMMA and poly(MEBIm-OH). For poly(MEBP-Br), after 168 h in 20 equiv KOH/D<sub>2</sub>O at 80 °C, evidence of significant hydrolysis is noted in the undegraded

cation peaks, as well as the peaks that arise due to the E2 elimination reaction; overall, 65.5% of the backbone undergoes hydrolysis (see Figures S9 and S10, Scheme S3). This could provide a potential explanation for the extraordinarily high chemical stability of poly(MEBP-Br), as the small molecule byproduct of hydrolysis may have higher resistance to hydroxide attack, keeping the pyrrolidinium ring intact. However, of the cations that remained tethered to the polymer backbone in 20 equiv KOH/D<sub>2</sub>O at 80 °C for 168 h, only 24.1% underwent E2 elimination; butylpyrrolidinium remains the most chemically stable polymeric cation of those considered. Ester hydrolysis was not identified as a primary mechanism of degradation in the ammonium-based PIL (see Figure S11).

## CONCLUSIONS

The alkaline chemical stability of PILs with various cations was examined with <sup>1</sup>H NMR spectroscopy in comparison with their analogous ionic salts. Results show enhanced chemical stability of imidazolium- and pyrrolidinium-based PILs relative to quaternary ammonium- and phosphonium-based PILs. Results for the ionic salts are in stark contrast to the PILs, as the imidazolium salts showed significantly more degradation than the quaternary ammonium and phosphonium salts at all conditions examined, while the pyrrolidinium-based salt showed no degradation equivalent to that of the ammonium- and phosphonium-based salts. Another inconsistency between salt and polymer was observed when comparing the two imidazolium cations; ionic salt results showed that methyl substitution in the C2 position significantly lessened degradation, while the PIL with unsubstituted imidazolium actually showed higher chemical stability under all conditions measured compared to its substituted PIL counterpart. Overall, the alkaline chemical stability of the free cations in solution investigated in this study showed no correlation to that of the

tethered cations on the PILs, suggesting that small molecule studies may not provide a solid basis for comparison of relative cation stability as a preliminary screening tool for determining the most promising cations.

## ■ ASSOCIATED CONTENT

### 📄 Supporting Information

The Supporting Information is available free of charge on the ACS Publications website at DOI: 10.1021/acs.macromol.5b01223.

Additional  $^1\text{H}$  NMR data (PDF)

## ■ AUTHOR INFORMATION

### Corresponding Author

\*E-mail: elabd@tamu.edu (Y.A.E.).

### Notes

The authors declare no competing financial interest.

## ■ ACKNOWLEDGMENTS

This work is supported in part by the U.S. Army Research Office under Grant W911NF-14-0310.

## ■ REFERENCES

- (1) Varcoe, J. R.; Slade, R. C. T. Prospects for Alkaline Anion-Exchange Membranes in Low Temperature Fuel Cells. *Fuel Cells* **2005**, *5*, 187–200.
- (2) Ye, Y.; Sharick, S.; Davis, E. M.; Winey, K. I.; Elabd, Y. A. High Hydroxide Conductivity in Polymerized Ionic Liquid Block Copolymers. *ACS Macro Lett.* **2013**, *2*, 575–580.
- (3) Nykaza, J. R.; Ye, Y.; Elabd, Y. A. Polymerized Ionic Liquid Diblock Copolymers with Long Alkyl Side-chain Length. *Polymer* **2014**, *55*, 3360–3369.
- (4) Ye, Y.; Elabd, Y. A. Relative Chemical Stability of Imidazolium-Based Alkaline Anion Exchange Polymerized Ionic Liquids. *Macromolecules* **2011**, *44*, 8494–8503.
- (5) Chen, D.; Hickner, M. A. Degradation of Imidazolium- and Quaternary Ammonium-Functionalized Poly(flourenyl ether ketone sulfone) Anion Exchange Membranes. *ACS Appl. Mater. Interfaces* **2012**, *4*, 5775–5781.
- (6) Qiu, B.; Lin, B.; Si, Z.; Qiu, L.; Chu, F.; Zhao, J.; Yan, F. Bis-imidazolium-based Anion-Exchange Membranes for Alkaline Fuel Cells. *J. Power Sources* **2012**, *217*, 329–335.
- (7) Ran, J.; Wu, L.; Varcoe, J. R.; Ong, A. L.; Poynton, S. D.; Xu, T. Development of Imidazolium-type Alkaline Anion Exchange Membranes for Fuel Cell Application. *J. Membr. Sci.* **2012**, *415*, 242–249.
- (8) Li, W.; Fang, J.; Lv, M.; Chen, C.; Chi, X.; Yang, Y.; Zhang, Y. Novel Anion Exchange Membranes Based on Polymerizable Imidazolium Salt for Alkaline Fuel Cell Applications. *J. Mater. Chem.* **2011**, *21*, 11340–11346.
- (9) Lin, B.; Dong, H.; Li, Y.; Si, Z.; Gu, F.; Yan, F. Alkaline Stable C2-Substituted Imidazolium-Based Anion-Exchange Membranes. *Chem. Mater.* **2013**, *25*, 1858–1867.
- (10) Gu, F.; Dong, H.; Li, Y.; Si, Z.; Yan, F. Highly Stable N3-Substituted Imidazolium-Based Alkaline Anion Exchange Membranes: Experimental Studies and Theoretical Calculations. *Macromolecules* **2014**, *47*, 208–216.
- (11) Qiu, B.; Lin, B.; Qiu, L.; Yan, F. Alkaline Imidazolium- and Quaternary Ammonium-Functionalized Anion Exchange Membranes for Alkaline Fuel Cell Applications. *J. Mater. Chem.* **2012**, *22*, 1040–1045.
- (12) Zhang, F.; Zhang, H.; Qu, C. Imidazolium Functionalized Polysulfone Anion Exchange Membrane for Fuel Cell Application. *J. Mater. Chem.* **2011**, *21*, 12744–12752.
- (13) Nuñez, S. A.; Hickner, M. A. Quantitative  $^1\text{H}$  NMR Analysis of Chemical Stabilities in Anion-Exchange Membranes. *ACS Macro Lett.* **2013**, *2*, 49–52.
- (14) Vandiver, M. A.; Caire, B. R.; Poskin, Z.; Li, Y.; Seifert, S.; Knauss, D. M.; Herring, A. M.; Liberatore, M. W. Durability and Performance of Polystyrene-*b*-poly(vinylbenzyl trimethylammonium) Diblock Copolymer and Equivalent Blend Anion Exchange Membranes. *J. Appl. Polym. Sci.* **2015**, *132*, 41596.
- (15) Yan, J.; Hickner, M. A. Anion Exchange Membranes by Bromination of Benzylmethyl-Containing Poly(sulfone)s. *Macromolecules* **2010**, *43*, 2349–2356.
- (16) Tsai, T.-H.; Maes, A. M.; Vandiver, M. A.; Versek, C.; Seifert, S.; Tuominen, M.; Liberatore, M. W.; Herring, A. M.; Coughlin, E. B. Synthesis and Structure–conductivity Relationship of Polystyrene-*block*-poly(vinyl benzyl trimethylammonium) for Alkaline Anion Exchange Membrane Fuel Cells. *J. Polym. Sci., Part B: Polym. Phys.* **2013**, *51*, 1751–1760.
- (17) Sturgeon, M. R.; Macomber, C. S.; Engtrakul, C.; Long, H.; Pivovar, B. S. Hydroxide based Benzyltrimethylammonium Degradation: Quantification of Rates and Degradation Technique Development. *J. Electrochem. Soc.* **2015**, *162*, F366–F372.
- (18) Choe, Y.-K.; Fujimoto, C.; Lee, K.-S.; Dalton, L. T.; Ayers, K.; Henson, N. J.; Kim, Y. S. Alkaline Stability of Benzyl Trimethyl Ammonium Functionalized Polyaromatics: A Computational and Experimental Study. *Chem. Mater.* **2014**, *26*, 5675–5682.
- (19) Chen, D.; Hickner, M. A. Ion Clustering in Quaternary Ammonium Functionalized Benzylmethyl Containing Poly(arylene ether ketone)s. *Macromolecules* **2013**, *46*, 9270–9278.
- (20) Hibbs, M. R. Alkaline Stability of Poly(phenylene)-based Anion Exchange Membranes with Various Cations. *J. Polym. Sci., Part B: Polym. Phys.* **2013**, *51*, 1736–1742.
- (21) Arges, C. G.; Ramani, V. Investigation of Cation Degradation in Anion Exchange Membranes Using Multi-Dimensional NMR Spectroscopy. *J. Electrochem. Soc.* **2013**, *160*, F1006–F1021.
- (22) Arges, C. G.; Ramani, V. Two-dimensional NMR Spectroscopy Reveals Cation-triggered Backbone Degradation in Polysulfone-based Anion Exchange Membranes. *Proc. Natl. Acad. Sci. U. S. A.* **2013**, *110*, 2490–2495.
- (23) Arges, C. G.; Kulkarni, S.; Baranek, A.; Pan, K.-J.; Jung, M.-S.; Patton, D.; Mauritz, K. A.; Ramani, V. Quarternary Ammonium and Phosphonium Based Anion Exchange Membranes for Alkaline Fuel Cells. *ECS Trans.* **2010**, *33*, 1903–1913.
- (24) Noonan, K. J. T.; Hugar, K. M.; Kostalik, H. A.; Lobkovsky, E. B.; Abruña, H. D.; Coates, G. W. Phosphonium-Functionalized Polyethylene: A New Class of Base-Stable Alkaline Anion Exchange Membranes. *J. Am. Chem. Soc.* **2012**, *134*, 18161–18164.
- (25) Gu, S.; Cai, R.; Luo, T.; Chen, Z.; Sun, M.; Liu, Y.; He, G.; Yan, Y. A Soluble and Highly Conductive Ionomer for High-Performance Hydroxide Exchange Membrane Fuel Cells. *Angew. Chem., Int. Ed.* **2009**, *48*, 6499–6502.
- (26) Wang, J.; Li, S.; Zhang, S. Novel Hydroxide-Conducting Polyelectrolyte Composed of an Poly(arylene ether sulfone) Containing Pendant Quaternary Guanidinium Groups for Alkaline Fuel Cell Applications. *Macromolecules* **2010**, *43*, 3890–3896.
- (27) Liu, L.; Li, Q.; Dai, J.; Wang, H.; Jin, B.; Bai, R. A Facile Strategy for the Synthesis of Guanidinium-functionalized Polymer as Alkaline Anion Exchange Membrane with Improved Alkaline Stability. *J. Membr. Sci.* **2014**, *453*, 52–60.
- (28) Kim, D. S.; Labouriau, A.; Guiver, M. D.; Kim, Y. S. Guanidinium-Functionalized Anion Exchange Polymer Electrolytes via Activated Fluorophenyl-Amine Reaction. *Chem. Mater.* **2011**, *23*, 3795–3797.
- (29) Sajjad, S. D.; Hong, Y.; Liu, F. Synthesis of Guanidinium-based Anion Exchange Membranes and their Stability Assessment. *Polym. Adv. Technol.* **2014**, *25*, 108–116.
- (30) Gu, F.; Dong, H.; Li, Y.; Sun, Z.; Yan, F. Base Stable Pyrrolidinium Cations for Alkaline Anion Exchange Membrane Applications. *Macromolecules* **2014**, *47*, 6740–6747.
- (31) Price, S. C.; Williams, K. S.; Beyer, F. L. Relationships between Structure and Alkaline Stability of Imidazolium Cations for Fuel Cell Membrane Applications. *ACS Macro Lett.* **2014**, *3*, 160–165.

(32) Thomas, O. D.; Soo, K. J. W. Y.; Peckham, T. J.; Kulkarni, M. P.; Holdcroft, S. A Stable Hydroxide-Conducting Polymer. *J. Am. Chem. Soc.* **2012**, *134*, 10753–10756.

(33) Ye, Y.; Elabd, Y. A. Anion Exchanged Polymerized Ionic Liquids: High Free Volume Single Ion Conductors. *Polymer* **2011**, *52*, 1309–1317.

(34) Yuesheng, Y.; Elabd, Y. A. Chemical Stability of Anion Exchange Membranes for Alkaline Fuel Cells. In *Polymers for Energy Storage and Delivery: Polyelectrolytes for Batteries and Fuel Cells*; ACS Symposium Series 1096; American Chemical Society: Washington, DC, 2012; Vol. 1096, pp 233–251.

(35) Hofmann, A. W.; Cahours, A. *Philos. Trans. R. Soc. London* **1857**, *147*, 575.

(36) Zanger, M.; Vander Werf, C. A.; McEwen, W. E. Kinetic Study of the Decomposition of Quaternary Phosphonium Hydroxides. *J. Am. Chem. Soc.* **1959**, *81*, 3806–3807.

(37) Gaetjens, E.; Morawetz, H. Intramolecular Carboxylate Attack on Ester Groups. II. The Effect of Diastereoisomerism in Polymers and their Low Molecular Weight Models. *J. Am. Chem. Soc.* **1961**, *83*, 1738–1742.

(38) Baines, F. C.; Bevington, J. C. A Tracer Study of the Hydrolysis of Methyl Methacrylate and Methyl Acrylate Units in Homopolymers and Copolymers. *J. Polym. Sci., Part A-1: Polym. Chem.* **1968**, *6*, 2433–2440.